The Open Neuroimaging Journal
DOI: 10.2174/0118744400462276260902061351, 2026, 19, e18744400462276
ISSN: 1874-4400

RESEARCH ARTICLE **OPEN ACCESS**

Diffusion Tensor Imaging as a Preliminary Study of White Matter Associations with Surgical Outcome in Mesial Temporal Lobe Epilepsy

Ítalo César Porto Xavier[1,*], Fernando Cendes[1], Marina Koutsodontis Machado Alvim[1], Brunno Machado de Campos[1] and Clarissa Lin Yasuda[1]

[1]*Medical Sciences Faculty (FCM-UNICAMP), Neuroimaging Laboratory (Clinics Hospital of State University of Campinas), Campinas, Brazil*

Abstract:

Objective: This study evaluates pre-surgery white matter abnormalities in evaluating the association between pre-surgical white matter integrity and post-surgery outcomes at the group level using Diffusion Tensor Imaging (DTI) in patients with Mesial Temporal Lobe Epilepsy (MTLE), specifically examining the differences between seizure-free and non-seizure-free patients, by Regions of Interest (ROIs) and diffusion parameters (biomarkers).

Methods: A retrospective analysis was conducted on pre-surgical DTI data from MTLE patients who underwent amygdalohippocampectomy with the subject outcome evaluation. Key parameters, including fractional anisotropy (FA), mean diffusivity (MD), axial diffusion (AD), and radial diffusion (RD), were extracted from regions of interest (ROIs) such as the hippocampus, thalamus, and temporal pole. Statistical analysis included ANOVA with Bonferroni post-hoc tests to compare surgical responders and non-responders on the ipsilateral and contralateral sides of the epileptogenic zone, as per clinical convention.

Results: FA values in the contralateral hippocampus and thalamus were significantly lower in the Not-SF group compared to the SF group ($p< 0.05$). RD values in the contralateral hippocampus and temporal pole were significantly higher in the Not-SF group ($p< 0.05$). In ipsilateral regions, MD and RD values in the hippocampus and temporal pole were significantly higher in the Not-SF group ($p< 0.01$), while FA values were significantly lower ($p< 0.001$). AD did not show significant differences. Overall, increased RD and MD and reduced FA in the Not-SF group indicate reduced microstructural integrity associated with poor seizure control.

Discussion: This study demonstrates that diffusion-based structural connectivity analysis can distinguish seizure-free from non–seizure-free TLE patients, highlighting the clinical relevance of hippocampus–temporal pole and hippocampus–thalamus pathways in postoperative outcomes. By extending diffusion evaluation beyond traditional tracts and integrating modern segmentation and tractography tools, our findings support the role of TLE as a network disorder and emphasize the potential of advanced DTI methods for understanding the network-level changes associated with surgical outcomes.

Conclusion: This study shows that diffusion-based structural connectivity metrics, particularly within hippocampus–temporal pole and hippocampus–thalamus pathways, showed exploratory associations with surgical outcomes in MTLE patients. While these metrics suggest differences between outcome groups, these findings are hypothesis-generating.

Keywords: Epilepsy, Diffusion tensor imaging, Mesial temporal lobe epilepsy, Structural connectivity, Hippocampus, Thalamus, Temporal pole, Surgical outcome.

*Address correspondence to this author at the Medical Sciences Faculty (FCM-UNICAMP), Neuroimaging Laboratory (Clinics Hospital of State University of Campinas) Campinas, Brazil, MRI Sector - Rua Vital Brasil, 888, Hospital de Clínicas, 2º Piso - Cidade Universitária, Campinas - SP, 13083-888, Brasil; E-mail: italo.cesar11@gmail.com

Cite as: Xavier Í, Cendes F, Alvim M, de Campos B, Yasuda C. Diffusion Tensor Imaging as a Preliminary Study of White Matter Associations with Surgical Outcome in Mesial Temporal Lobe Epilepsy. Open Neuroimaging J, 2026; 19: e18744400462276. http://dx.doi.org/10.2174/0118744400462276260902061351

Received: January 13, 2026
Revised: May 19, 2026
Accepted: June 21, 2026
Published: September 04, 2026

1. INTRODUCTION

About 50 million people in the world suffer from epilepsy today, of whom 80% live in low- to middle-income countries. The cause of the disease is not known, but it is related to several insults such as brain trauma during birth, head injuries, tumors, brain infections, and genetic conditions. The classification of epilepsy includes focal, generalized, combined (focal and generalized), and unknown. Each of these results in syndromes with distinct behaviors and sensations for each individual [1]. About 60% of focal seizures originate in the temporal lobe, whereas surgery is an option for patients who are refractory to antiseizure medications [2]. The literature reveals that 64% of these patients, who undergo surgery, obtain seizure control with improvement of their quality of life [3]. Once the subject has undergone the surgical procedure, the result is classified of treatment according to seizure frequency, divided into four classifications, Engel I (seizure-free), Engel II (rare seizures, 3 per year), Engel III (valid improvement or greater than 80% reduction in seizure frequency), Engel IV (no improvement or less than 80% reduction in seizure frequency) [4]. MTLE (Mesial Temporal Lobe Epilepsy) is a focal epilepsy that involves mesial structures of the temporal lobe.

1.1. DTI and its Importance

A type of MRI (Magnetic Resonance Imaging) protocol, called Diffusion Imaging, obtains diffusion data from the diffusion anisotropy of water molecules moving through microstructures that hinder neuronal communication. From diffusion data, it is possible to obtain a quantitative parameter indicating whether the structure is well-established and hindered.

These parameters, such as FA (Fractional Anisotropy), which is more commonly used and quantifies how strongly directional the local tract structure is, are related to the quantification of the mobility of water molecules in a voxel at an anisotropic level if close to 1, and isotropic if close to 0. It also obtains the AD (Axial Diffusion) related to the parallel direction, RD (Radial Diffusion) related to the transverse direction, and MD (Mean Diffusivity) related to the mean of axial and radial components. With the effects of anisotropy and water diffusion, biomarkers can measure various tissue characteristics, including myelination, axon diameter, fiber density, and fiber organization. However, it is important to reinforce that such biomarkers should be interpreted with caution [5-7].

However, diffusion metrics such as FA, RD, AD, and MD are not specific to single microstructural properties and should be interpreted cautiously, as they reflect a combination of biological factors, including myelination, axonal density, and fiber organization, as previously discussed in the literature [8].

DTI is a technique for primarily mapping white matter, with tensor adjustment at each voxel in the brain. Once this is done, it is possible to assess the orientation of the white fiber tracts and the strength of this directionality. Increasing the number of diffusion encoding gradients in the MRI protocol results in better resolution and a greater number of white matter tracts in that voxel. Tractography is the ability to graphically obtain the approximate representation of the white matter tracts. It is important for inferring connected structures (fascicles) and can be useful for making decisions in surgical operations. It results from a deterministic processing of DTI data [9-15]. It is important to consider that although tractography is capable of inferring connectivity effectively, it does not guarantee anatomical connection by itself [16].

There is a vast literature on structural connectivity analysis using DTI, assessing the integrity of isolated and known fascicles, such as the fornix, uncinate fasciculus, arcuate fasciculus, corpus callosum, fibers that are associative, projective, and commissural [17], in various diseases, such as in epilepsy [18-20], bipolar disorder [21], and tumors [22]. Recent works using high-resolution DTI have shown significant asymmetries in superficial and deep white matter, particularly involving the cingulum, uncinate fasciculus, and thalamic projections [23, 24]. However, there are still a few investigations into the analysis of predefined structures independent of known neural pathways and their correlation with clinical implications and surgical outcomes.

The use of Diffusion Tensor Imaging (DTI) to investigate structural biomarkers of neurological pathologies represents a promising and actively explored approach for assessing memory deficits [8]. Therefore, we aim to further advance this research project.

1.2. A Network Disease

It is suggested that the thalamus, mainly through the thalamocortical pathways, participates in TLE, which can be indirectly evaluated by EEG (electroencephalography) [25, 26], volumetric analysis [27], functional analysis [28], and that this pathway is confirmed by structural analysis [29]. Even with evidence not much clearer in the face of pathology, the temporal pole is also seriously affected in MTLE [30]. It was noted that the amygdala plays a significant role in the propagation of specific seizures [31]. The hippocampal structure is the region that is most affected in this type of epilepsy, and hippocampal sclerosis is the most frequent etiology for drug-resistant patients [32]. In terms of hippocampal functionality, it was found that TLE not only affects declarative memory but also performance in short-term verbal and visual memory, long-term verbal and visual memory, and working memory [33, 34]. Also in TLE, the thalamus volume, ipsilateral to seizure onset, was significantly decreased compared to controls [35]. In view of these investigations, we chose these three ROIs to be evaluated for structural connectivity with the hippocampus.

Recent diffusion and connectome-based studies support the characterization of Mesial Temporal Lobe Epilepsy (MTLE) as a disorder of distributed brain networks rather than a purely focal hippocampal lesion. Large-scale DTI analyses and graph-theoretical work have shown widespread white-matter disruption, reduced network efficiency, and altered hub integrity across limbic, temporal, and subcortical systems in patients with

TLE. These convergent findings imply that microstructural network compromise contributes to seizure propagation and clinical heterogeneity in MTLE [36, 23, 37, 38].

It is therefore of great use for the interpretation of neurological pathologies, such as epilepsy, to identify microstructural differences compared to healthy subjects, knowing that it is a network disease [36, 23].

Recent work integrating structural brain abnormalities with outcomes of deep brain stimulation has demonstrated that both focal and generalized epilepsies are embedded within reproducible and disease-specific network architectures, highlighting the relevance of network integrity for therapeutic response [39]. In parallel, advances in neuromodulation strategies, including deep brain stimulation, responsive neurostimulation, and vagus nerve stimulation, have further emphasized that successful seizure control often depends on modulating key nodes and connections within epileptogenic networks rather than targeting isolated lesions [40]. Together, these findings support the pursuit of imaging-based biomarkers capable of capturing network-level alterations relevant to prognosis and treatment selection in patients undergoing epilepsy surgery.

In addition, recent evidence suggests that network plasticity plays a key role in epilepsy, with structural and functional reorganization influencing clinical outcomes and treatment response [41].

It is reasonable to evaluate white matter structural connectivity using DTI in MTLE patients with seizure control and those without. The main hypothesis of this study was that there would be quantitative differences in structural connectivity in strategic regions of interest between these two groups of patients. This research is a preliminary study aimed at investigating group-level associations between diffusion metrics and surgical outcomes, identifying potential markers of microstructural damage.

2. MATERIALS AND METHODS

2.1. Study Design

This study is a retrospective cohort study designed to investigate the association between Diffusion Tensor Imaging (DTI) metrics and surgical outcomes in patients with mesial temporal lobe epilepsy with hippocampal sclerosis. The duration of the study comprised the period from August 2022 to January 2025.

2.2. Inclusion and Exclusion Criteria

Inclusion criteria correspond to adult patients diagnosed with Mesial Temporal Lobe Epilepsy (MTLE) associated with hippocampal sclerosis, patients who underwent standard surgical treatment (selective amygdalohippocampectomy), availability of preoperative and postoperative diffusion MRI scans, and a minimum postoperative follow-up sufficient for reliable Engel classification. The exclusion criteria include: presence of dual pathology or other structural abnormalities unrelated to MTLE; history of neurosurgical procedures prior to MTLE surgery; poor-quality or incomplete MRI datasets that prevent accurate diffusion analysis; and comorbid neurological or systemic disorders that could confound diffusion metrics.

A retrospective of MTLE patients who underwent amygdalohippocampectomy was analyzed. The sample group consisted of 77 patients divided into two groups. The first group consisted of controlled, seizure-free patients (Seizure Free), considered Engel Ia (SF) of 43 patients, and the second group consisted of the remainder of the classifications (Engel classes II, III, and IV), Not-SF (Not Seizure Free) of 34 patients. This grouping reflects clinical reality, where the primary therapeutic goal is complete seizure freedom (Engel I), given that even rare seizures (Engel II) significantly impact a patient's quality of life, legal capacity to drive, and psychosocial stability. The control group (CTRL) comprised 76 healthy subjects. The demographics for each group was as follows: SF, mean age 43.25 ± 9.91 (mean ± standard deviation), 23 females, 20 males; Not-SF, mean age 41.91 ± 11.80 (mean ± standard deviation), 17 females, 17 males; and CTRL, mean age 33.25 ± 11.96 years (mean ± standard deviation), 35 females, 41 males, shown in Table **1**. In total, 153 data points of the subjects, including the control and patient groups, were processed.

Table 1. Demographics of the subjects in the study.

Variable	Male	Female	Age
Not-SF	17	17	41.91 ± 11.80
SF	20	23	43.25 ± 9.91
CTRL	41	35	33.25 ± 11.96
p-value	$p<0.001$	$p<0.001$	$p<0.001$

Regarding seizure lateralization, 44 patients presented left-sided epilepsy and 33 patients presented right-sided epilepsy.

2.3. MRI Acquisition and Processing

Structural images were collected using T1-weighted acquisition, 1 mm^3 isotropic voxel, gapless, flip angle, TE/TR 3.2/7 ms, 180 sagittal slices with a FOV of 240 x 240. Diffusion images for the tractography and diffusion quantifications were acquired *via* planar echo imaging (EPI) with 2 mm^3 isotropic voxels, interpolated to 1x1x2 mm^3, rebuilt in a 256x256 matrix, 70 slices, TE/TR 61/8,500 ms, 90° flip angle, 32 directions from gradients, no averages, maximum b-factor 1,000 s/mm^2. For the patients, preoperative structural and diffusion data were selected.

Performing post-processing individually (for each subject) would be arduous and time-consuming, diverting user attention, so a loop program was developed in command lines to perform all data manipulation without the user being effectively present.

The first stage of the processing in the structural image was the extraction of the brain surface using a subroutine of the SPM12 Matlab Toolbox software [42].

The realization of corrections of non-uniformities, classification of the tissue type, labeling of the brain, internal and external masks, and the generation of the surface was carried out *via* command by the CSE (Cortical Surface Extraction) module [43] of the software BrainSuite. The BCI-DNI atlas [44] was used, whose protocol outlines 26 grooves for the recognition of 95 ROIs (Regions of Interest), including cerebral gyri and some subcortical structures, for co-registration.

The second stage refers to the diffusion data, where the eddy module of the FSL (FMRIB Software Library) software [45] is used for motion correction and signal drop due to distortion. Knowing that the operating system was Windows (FSL only for Linux systems), to perform this remediation step, the DSI Studio program was used, which includes a correction module for the Windows system developed by the author (http://dsi-studio.labsolver.org) [46]. It was set to 0 1 0 0.1 for the acquisition parameter (phase encoding direction) for eddy current and susceptibility. The tensor processing step and geometric distortion correction for the T1 image, this vector image, and intravoxel magnitude were performed using the BDP (BrainSuite Diffusion Pipeline) [47]. In this step, we set the FA threshold to 0.2, 1.25 seeds per voxel, an angle threshold of 30 degrees, and a step size of 0.5mm.

In the tractography stage, the analysis of white matter and connectivity between two ROIs was processed using MATLAB's TractConnect Toolbox [48] to obtain diffusion parameters in strategic regions of interest, based on the surface generated by the tractography. The streamlines were not manually selected but were auto-generated and output by the algorithm based on seed regions between the two surfaces' ROIs, the diffusion map file, and the surface-registered atlas as input.

The overview of the post-processing stages of the data is shown in Fig. (**1**), and an automated code (https://github.com/italoxaviercp/Structural-Connectivity-DTI-Multi-Tools) was used.

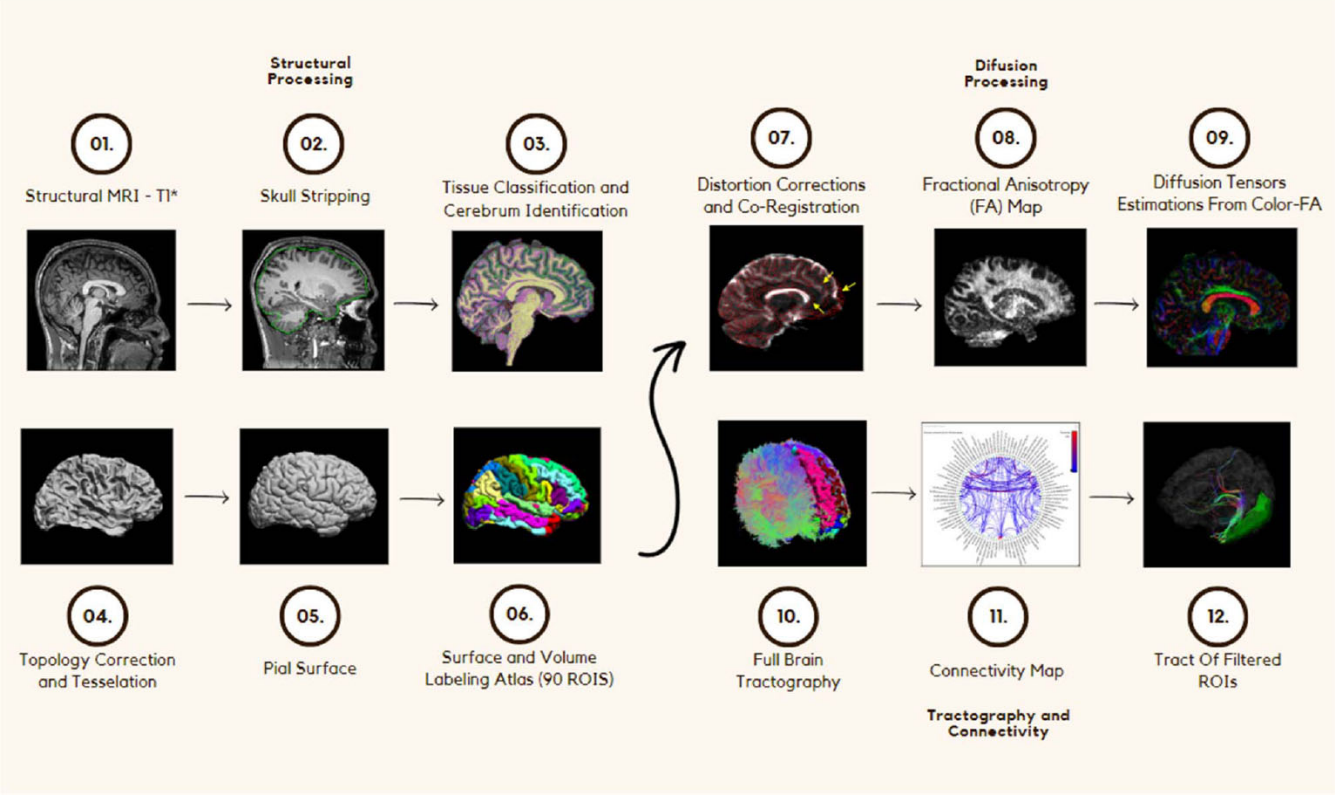

Fig. (1). (01) High-resolution structural T1-weighted MRI acquisition used as anatomical reference. (02) Skull stripping procedure for removal of non-brain tissues. (03) Tissue classification and cerebral structure identification, enabling separation of gray matter, white matter, and cerebrospinal fluid. (04) Topological correction and cortical surface tessellation to ensure anatomical consistency. (05) Reconstruction of the pial surface representing the outer boundary of the cerebral cortex. (06) Surface and volumetric labeling based on an anatomical atlas, defining 90 regions of interest (ROIs). (07) Correction of diffusion data distortions and co-registration between diffusion and structural images. (08) Generation of diffusion maps, including fractional anisotropy (FA), axial diffusivity (AD), radial diffusivity (RD), and mean diffusivity (MD). (09) Estimation of diffusion tensors and orientation information derived from color-encoded FA maps. (10) Whole-brain tractography performed in individual subject space. (11) Construction of connectivity matrices representing structural connections between atlas-defined ROIs. (12) Extraction and filtering of tracts connecting selected ROIs, enabling quantitative analysis of diffusion parameters along specific pathways.

2.4. Statistical Analysis

For statistical analyses, the RStudio software was used. A total of 20 primary ANOVA tests were performed (covering 4 diffusion parameters across 5 ROI pairs). While Bonferroni correction was applied to all post-hoc comparisons to control for multiple pairwise tests, no global alpha correction was applied to the primary ANOVA results. A p-value < 0.05 was considered statistically significant for these exploratory analyses [49]. The statistical analysis aimed to consider the behavior of the FA, AD, RD, and MD parameters as a function of ROIs, among the CTRL, SF, and Not-SF groups, both as variables that suggest differences between the groups by region evaluated, and also as a measure that differentiates these same groups. From the volumetric surface of the white matter obtained in the processing, for all patients, among the selected ROIs, its lateralization was categorized by epileptogenic focus. That is, for those who underwent a surgical procedure on the left side, the evaluation of the parameters of the structures on the left side was considered the ipsilateral category (same side). In the same way, the data were reorganized on the right side. This organization of the columns facilitates the clinical interpretation of the results.

3. RESULTS

For visual evaluation of the tractography, some surfaces were rendered from the study between CTRL and a random patient. With total brain treatment and filtered ROI presentation, it was possible to verify a reduction in the number of fibers and voxels in white matter for a patient compared to a control. This difference was highlighted in the left hippocampus compared with the right hippocampus, in the hippocampus with the ipsilateral thalamus, and in the hippocampus with the ipsilateral temporal pole, as Fig. (2) illustrates.

For the structural connectivity between the left hippocampus and the right hippocampus, ANOVA indicated a significant difference between the groups (CTRL, SF, and Not-SF) by biomarker MD ([F(2,150) = 3.467; p = 0.0337]) (Fig. 3). The post-hoc of multiple comparisons using the Bonferroni method did not identify a significant difference between the groups.

For the structural connectivity between the Hippocampus and the Temporal Pole, Ipsilateral, the ANOVA indicated a significant difference between the groups through FA ([F(2,150) = 12.44; p = 1.01e-05]), RD ([F(2,150) = 11.65; p = 1.97e-05]) and MD ([F(2,150) = 8.31; p = 0.000377]) (Fig. 4). Post-hoc testing identified differences between CTRL and Not-SF groups (p = 1.3e-05) and the SF and Not-SF groups (p = 0.00019) for FA. The post-hoc test for RD found differences between the CTRL and Not-SF groups (p = 2.2e-05) and between the SF and Not-SF groups (p = 0.00043). The post-hoc test found differences between the CTRL and Not-SF groups (p = 0.00034) and between the SF and Not-SF groups (p = 0.00491) for MD. In these comparisons, the Not-SF group showed significantly lower FA and higher RD and MD values compared to the SF group, indicating reduced microstructural integrity in patients with poor seizure control.

For structural connectivity between the hippocampus and the temporal pole, contralateral ANOVA indicated a significant difference between the FA groups ([F(2,150) = 13.84; p = 3.05e-06]), RD ([F(2,150) = 14.43; p = 1.86e-06]), and MD ([F(2,150) = 9.517; p = 0.000129]) (Fig. 5). The post-hoc test identified differences between the CTRL and SF groups (p = 0.0169) and between CTRL and Not-SF (p = 2.6e-06) for FA. A difference was found between the Not-SF and SF groups (p = 0.0181) and the Not-SF and CTRL (p = 1.1e-06) for RD. The post hoc test identified a difference between the CTRL and Not-SF groups (p = 7.8e-05) for the MD.

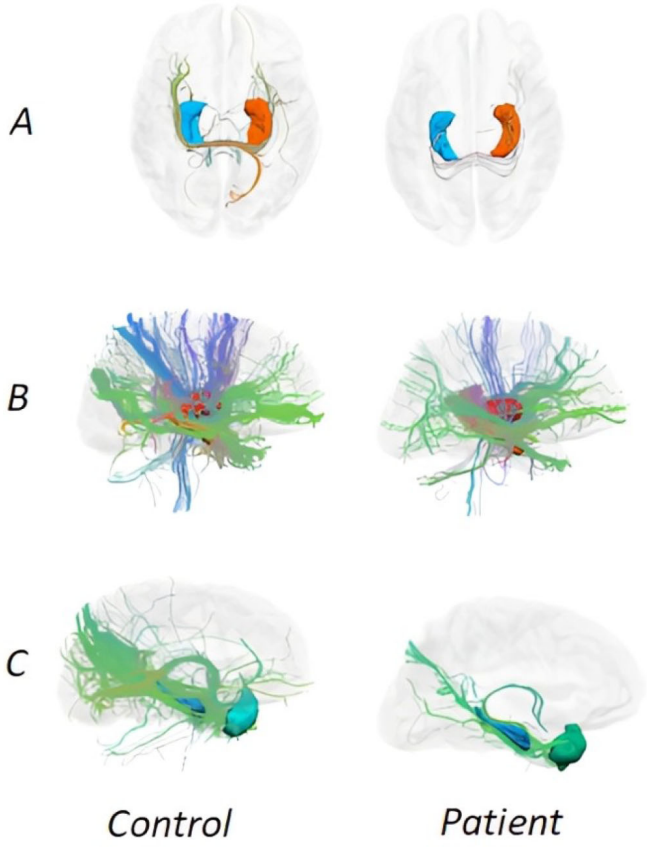

Fig. (2). Rendering of a control subject and a Not-SF patient subject. **A** - The Hippocampal and Hippocampal ROIs. Control presenting 435 of 1,675,966 total fibers and patient presenting 22 of 1,119,136 total fibers. **B** - Ipsilateral Hippocampal and Thalamus ROIs. Control showing 6,550 of 1,675,966 total fibers and patient, featuring 3,309 of 1,119,136 total fibers. **C** - Ipsilateral Hippocampus and Temporal Pole ROIs. Control, presenting 6,592 of 1,675,966 total fibers and patient, presenting 751 of 1,119,136 total fibers.

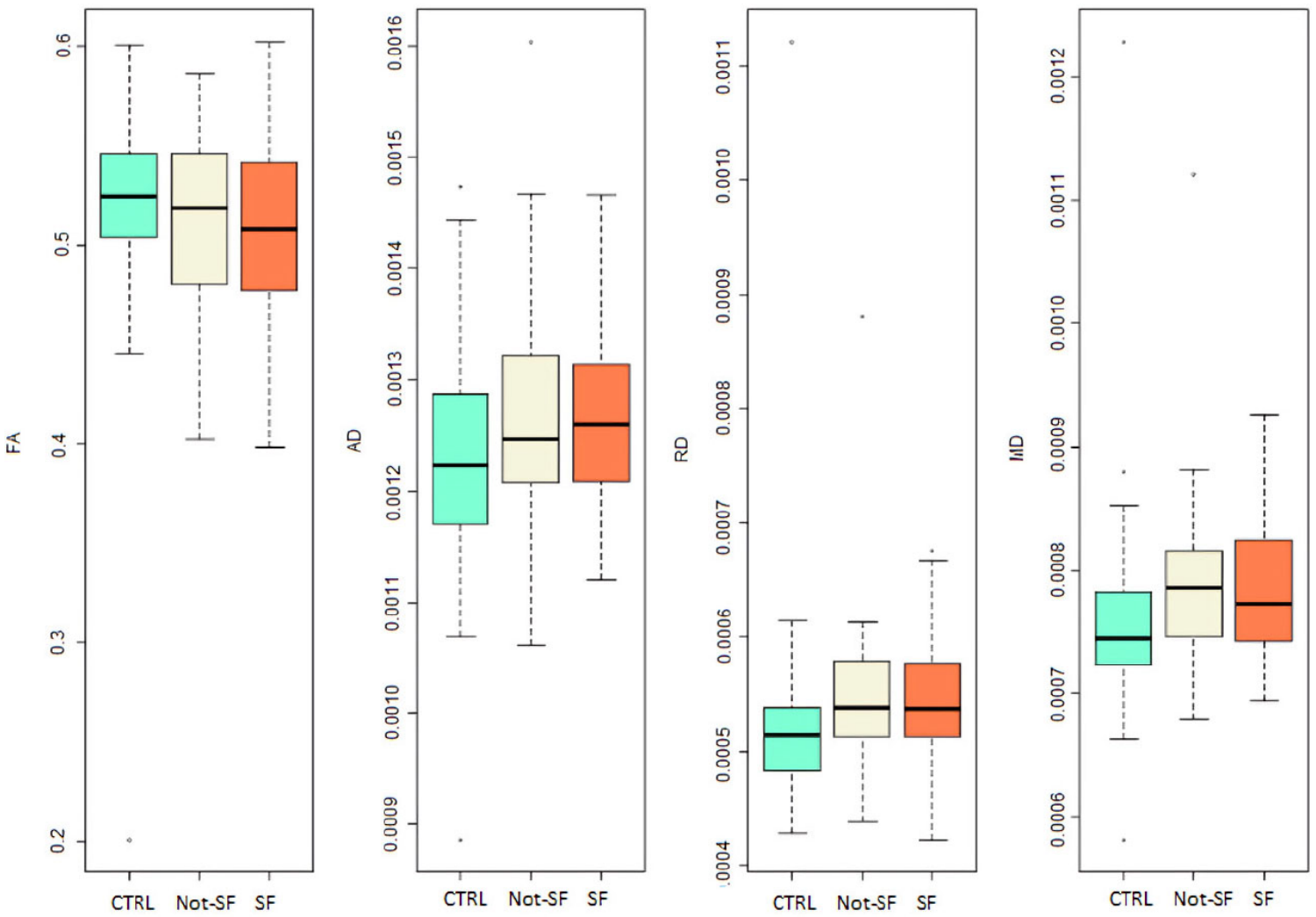

Fig. (3). Boxplots showing diffusion tensor imaging (DTI) metrics between the bilateral hippocampi, including fractional anisotropy (FA), axial diffusivity (AD), radial diffusivity (RD), and mean diffusivity (MD). Distributions are shown for healthy controls (CTRL, green), patients who achieved seizure freedom after surgery (SF, orange), and patients who did not achieve seizure freedom (Not-SF, cream). Boxes represent the interquartile range (IQR), central horizontal lines indicate the median, whiskers denote values within 1.5 × IQR, and dots indicate outliers. Group differences reflect variability in microstructural integrity of hippocampal interconnections as assessed by DTI metrics.

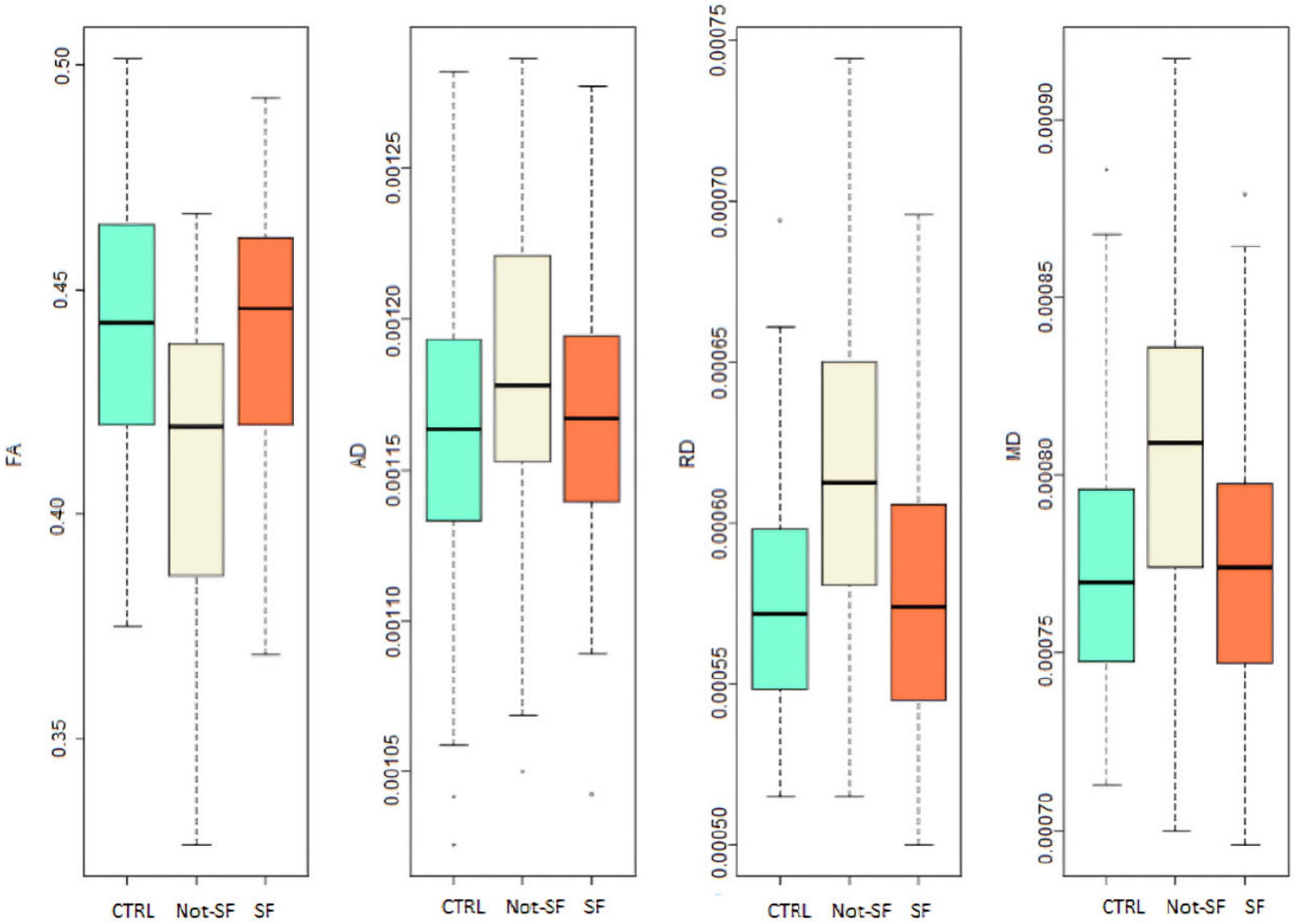

Fig. (4). Boxplots illustrating diffusion tensor imaging (DTI) metrics between the hippocampus and the temporal pole ipsilateral to the epileptogenic focus, including fractional anisotropy (FA), axial diffusivity (AD), radial diffusivity (RD), and mean diffusivity (MD). Results are shown for healthy controls (CTRL, green), patients who achieved postoperative seizure freedom (SF, orange), and patients who did not achieve seizure freedom (Not-SF, cream). Boxes represent the interquartile range (IQR), central lines indicate the median, whiskers correspond to values within 1.5 × IQR, and dots denote outliers. These distributions characterize microstructural differences in ipsilateral hippocampal–temporal pole connectivity among the studied groups.

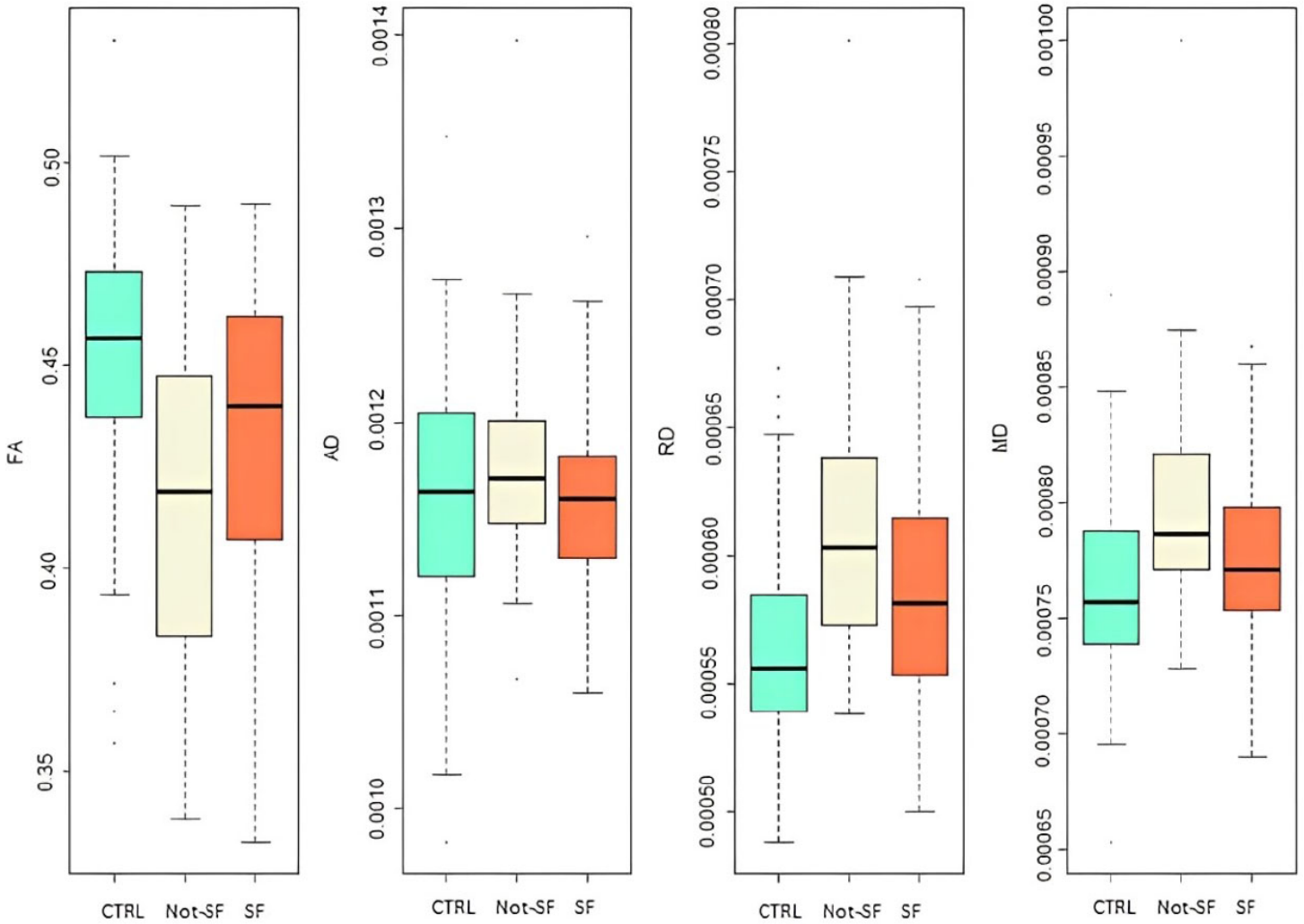

Fig. (5). Boxplots depicting diffusion tensor imaging (DTI) metrics between the hippocampus and the temporal pole contralateral to the epileptogenic focus, including fractional anisotropy (FA), axial diffusivity (AD), radial diffusivity (RD), and mean diffusivity (MD). Data are presented for healthy controls (CTRL, green), patients who achieved seizure freedom following surgery (SF, orange), and patients who did not achieve seizure freedom (Not-SF, cream). Boxes indicate the interquartile range (IQR), horizontal lines represent the median, whiskers extend to 1.5 × IQR, and dots identify outliers. These distributions reflect microstructural properties of contralateral hippocampal–temporal pole connectivity across the studied groups.

For the structural connectivity between Hippocampus and Thalamus, Ipsilateral, ANOVA indicated a significant difference between the groups through the FA ([F(2,150) = 22.85; p = 2.18e-09]), AD ([F(2.150) = 3.095; p = 0.0482]), RD ([F(2.150) = 25.56; p = 2.8e-10]) and MD ([F(2.150) = 17.26; p = 1.8e-07]) (Fig. **6**). The post-hoc test identified differences between the CTRL and Not-SF groups (p = 1.4e-07) and the CTRL and SF groups (p = 1.4e-06) for FA. No difference was found between the groups for AD. The Post-Hoc Test for RD found differences between the CTRL and Not-SF groups (p = 1.0e-08) and between the CTRL and SF groups (p = 1.2e-06). The post-hoc test found differences between the CTRL and SF groups (p = 0.00012) and between CTRL and Not-SF (p = 1.5e-06) for MD. Not-SF patients presented lower FA and higher RD and MD values compared to SF patients, consistent with greater microstructural disruption in this group.

For structural connectivity between Hippocampus and Thalamus, Contralateral, ANOVA indicated a significant difference between the groups through the FA ([F(2,150) = 17.54; p = 1.43e-07]), RD ([F(2,150) = 16.63; p = 3.01e-07]) and MD ([F(2,150) = 9.591; p = 0.00012]) (Fig. **7**). The post-hoc test identified differences between the CTRL and Not-SF groups (p = 1.2e-07), the SF and Not-SF groups (p = 0.0318), and the CTRL and SF groups (p = 0.0061) for FA. The post-hoc test for RD found differences between the CTRL and Not-SF groups (p = 8.5e-07) and between the CTRL and SF groups (p = 0.00073). Post-hoc testing found differences between CTRL and SF groups (p = 0.00473) and between CTRL and Not-SF (p = 0.00048) for MD. Comparisons between SF and Not-SF groups indicate that the Not-SF group generally exhibited lower FA and higher RD values, suggesting persistent contralateral microstructural alterations associated with poor surgical outcome.

The results of ANOVA are presented in Table **2**, showing that the MD parameter was able to identify significant differences between the groups for each pair of connected regions, and that the AD parameter was not useful for this context in any condition. On the other hand, the FA and RD parameters just weren't useful for identifying differences in the region connecting the two hippocampi. The results of the multiple-comparison test to verify where the difference between the groups lies are presented in Table **3**.

4. DISCUSSION

4.1. Brain Structure

White matter changes in TLE primarily affect the ipsilateral hemisphere and temporal lobe, with no structural abnormalities in extra-temporal regions. Differences exist between patients who became seizure-free after surgical treatment and those who did not, including surgical treatment, behavioral and neuropsychological characteristics, and diffusion data, suggesting microscopic structural distinctions.

There is evidence of hippocampal-thalamic spatial connectivity using structural data [29], reinforcing the involvement of medial structures in altered emotional reactions, as suggested by Papez's circuit [50]. Structural connectivity between the hippocampus and temporal pole has also been evaluated [37]. To our knowledge, few studies have analyzed diffusion data in white matter surfaces linking the hippocampus, thalamus, and temporal pole in TLE patients with hippocampal sclerosis post-surgery.

A key distinction of this study is that diffusion analysis in TLE is not restricted to known tracts such as the uncinate fasciculus, arcuate fasciculus, cingulum, external capsule, or fornix [51]. It extends to any regional fiber connecting affected structures, including extratemporal and limbic tracts like the optic radiation [52].

Within this network-based framework, the present findings gain particular relevance. Alterations in diffusion metrics along hippocampal–temporal pole and hippocampal–thalamic pathways suggest that microstructural integrity of limbic and subcortical connections may influence postoperative seizure control. These pathways are central to seizure propagation and modulation, and their involvement is consistent with recent large-scale network models derived from structural abnormalities and neuromodulation targets in epilepsy [39]. Importantly, emerging molecular evidence indicates that drug-resistant epilepsies share convergent disruptions in gene regulatory networks across brain regions, reinforcing the concept that epilepsy-related dysfunction extends beyond the primary epileptogenic zone [53, 26]. In this context, diffusion-based biomarkers may capture downstream structural consequences of these multilevel network alterations, offering potential markers that reflect group-level differences in surgical response.

4.2. Processing

DTI has proven to be an innovative tool, particularly for epilepsy cases with no clear structural abnormalities. Our processing was conducted similarly to studies on chronic anemia [54], evaluating intra-hemispheric structural connectivity in cortical and subcortical regions ipsilateral and contralateral to the epileptogenic focus. This differs from traditional analyses of individual structures or specific tracts [18, 51, 55-59] in TLE.

Unlike previous studies, this research integrated multiple modern tools: automatic cortical segmentation (SVReg), full brain tractography (Brainsuite), and ROI filtering (Tract Connect *via* Matlab). This ensured a preliminary statistical analysis with fine-tuned control over processing.

There is a lack of prior studies analyzing hippocampal connectivity to other cortical and subcortical regions through diffusion parameters following TLE surgery. This allowed for a more precise structural connectivity assessment, suggesting that this approach may offer additional insights in this context.

Table 2. ANOVA for ROIs and diffusion parameters.

ROI 1	ROI 2	fFA	pFA	fAD	pAD	fRD	pRD	fMD	pMD
Hippocampus (Left)	Hippocampus (Right)	0.879	0.433	2.696	0.0707	2.5	0.0853	3.467	0.0337
Hippocampus (Ipsilateral)	Thalamus (Ipsilateral)	12.44	1.01E-05	1.101	0.335	11.65	1.97E-05	8.311	0.000377
Hippocampus (Contralateral)	Thalamus (Ipsilateral)	13.84	3.05E-06	0.748	0.475	14.43	1.86E-06	9.517	0.000129
Hippocampus (Ipsilateral)	Temporal Pole (Ipsilateral)	22.85	2.18E-09	3.095	0.0482	25.56	2.80E-10	17.26	1.80E-07
Hippocampus (Contralateral)	Temporal Pole (Ipsilateral)	17.54	1.43E-07	2.016	0.137	16.63	3.01E-07	9.591	0.00012

Table 3. Bonferroni's post-hoc test, for multiple comparisons, indicating the significant differences in variances between the seizure-free (SF) and not-seizure-free groups (Not-SF).

ROIs	Diffusion Parameter	Group Comparison	Significance ($p<0.05$)
Hippo.-Hippo.	MD	CTRL *vs.* SF	0.11
Hippo.-Hippo.	MD	CTRL *vs.* Not-SF	0.0899
Hippo.-Hippo.	MD	SF *vs.* Not-SF	1
Hippo.-Temp.Pole (ipsi)	FA	CTRL *vs.* SF	1
Hippo.-Temp.Pole (ipsi)	FA	CTRL *vs.* Not-SF	1.30E-05
Hippo.-Temp.Pole (ipsi)	FA	SF *vs.* Not-SF	0.00019
Hippo.-Temp.Pole (ipsi)	RD	CTRL *vs.* SF	1
Hippo.-Temp.Pole (ipsi)	RD	CTRL *vs.* Not-SF	2.20E-05
Hippo.-Temp.Pole (ipsi)	RD	SF *vs.* Not-SF	0.00043
Hippo.-Temp.Pole (ipsi)	MD	CTRL *vs.* SF	1
Hippo.-Temp.Pole (ipsi)	MD	CTRL *vs.* Not-SF	0.00034
Hippo.-Temp.Pole (ipsi)	MD	SF *vs.* Not-SF	0.00491
Hippo.-Temp.Pole (contra)	FA	CTRL *vs.* SF	0.0169
Hippo.-Temp.Pole (contra)	FA	CTRL *vs.* Not-SF	2.60E-06
Hippo.-Temp.Pole (contra)	FA	SF *vs.* Not-SF	0.0726
Hippo.-Temp.Pole (contra)	RD	CTRL *vs.* SF	0.0511
Hippo.-Temp.Pole (contra)	RD	CTRL *vs.* Not-SF	1.10E-06
Hippo.-Temp.Pole (contra)	RD	SF *vs.* Not-SF	0.0181
Hippo.-Temp.Pole (contra)	MD	CTRL *vs.* SF	0.1945
Hippo.-Temp.Pole (contra)	MD	CTRL *vs.* Not-SF	7.80E-05
Hippo.-Temp.Pole (contra)	MD	SF *vs.* Not-SF	0.0593
Hippo.-Thal. (ipsi)	FA	CTRL *vs.* SF	1.40E-06
Hippo.-Thal. (ipsi)	FA	CTRL *vs.* Not-SF	1.40E-07
Hippo.-Thal. (ipsi)	FA	SF *vs.* Not-SF	1
Hippo.-Thal. (ipsi)	AD	CTRL *vs.* SF	0.3797
Hippo.-Thal. (ipsi)	AD	CTRL *vs.* Not-SF	0.059
Hippo.-Thal. (ipsi)	AD	SF *vs.* Not-SF	1
Hippo.-Thal. (ipsi)	RD	CTRL *vs.* SF	1.20E-06
Hippo.-Thal. (ipsi)	RD	CTRL *vs.* Not-SF	1.00E-08
Hippo.-Thal. (ipsi)	RD	SF *vs.* Not-SF	0.6515
Hippo.-Thal. (ipsi)	MD	CTRL *vs.* SF	0.00012
Hippo.-Thal. (ipsi)	MD	CTRL *vs.* Not-SF	1.50E-06
Hippo.-Thal. (ipsi)	MD	SF *vs.* Not-SF	0.68588
Hippo.-Thal. (contra)	FA	CTRL *vs.* SF	0.0061
Hippo.-Thal. (contra)	FA	CTRL *vs.* Not-SF	1.20E-07
Hippo.-Thal. (contra)	FA	SF *vs.* Not-SF	0.0318
Hippo.-Thal. (contra)	RD	CTRL *vs.* SF	0.00073
Hippo.-Thal. (contra)	RD	CTRL *vs.* Not-SF	8.50E-07
Hippo.-Thal. (contra)	RD	SF *vs.* Not-SF	0.26987
Hippo.-Thal. (contra)	MD	CTRL *vs.* SF	0.00473
Hippo.-Thal. (contra)	MD	CTRL *vs.* Not-SF	0.00048
Hippo.-Thal. (contra)	MD	SF *vs.* Not-SF	1

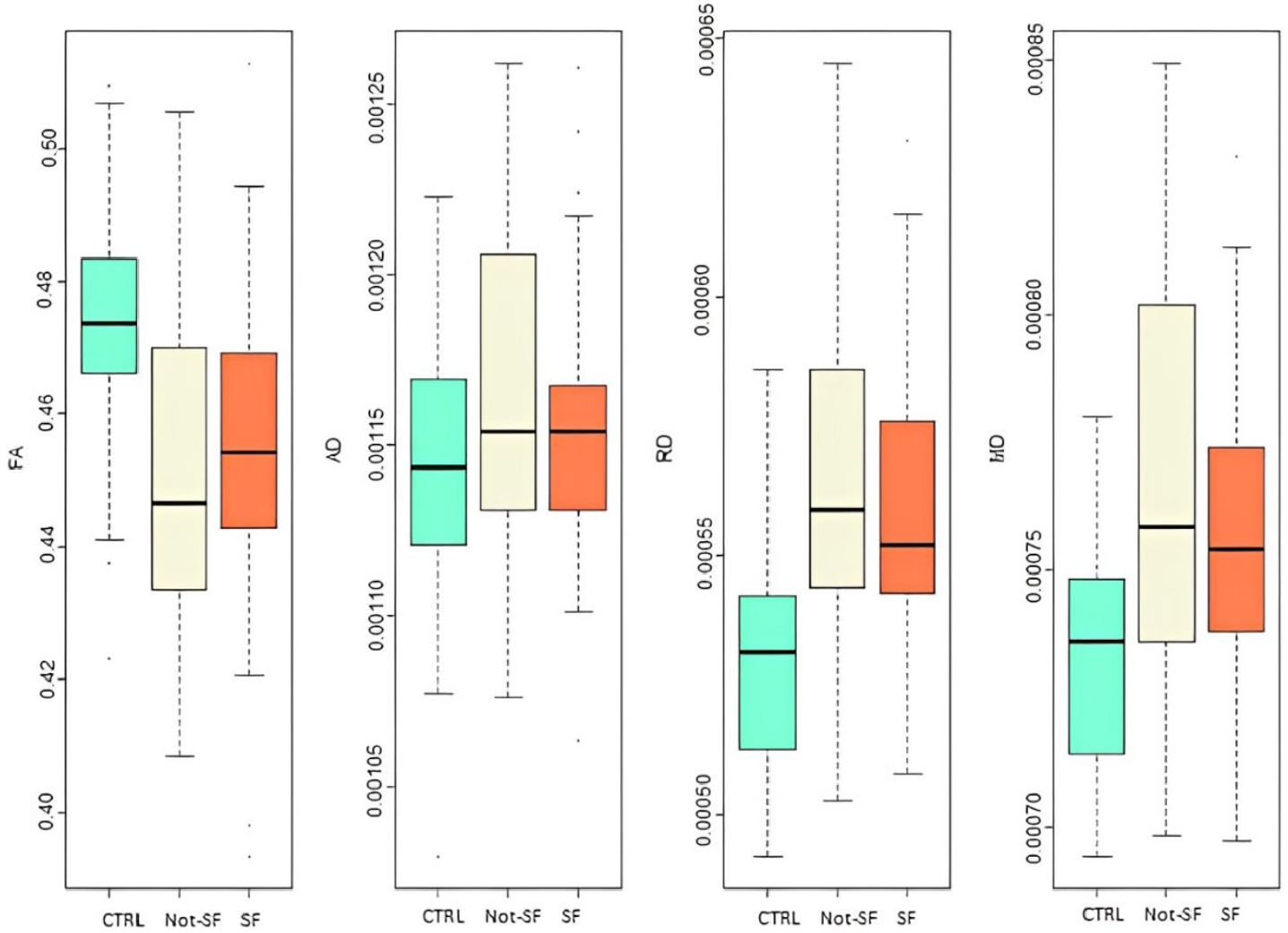

Fig. (6). Boxplots illustrating diffusion tensor imaging (DTI) metrics between the hippocampus and the thalamus ipsilateral to the epileptogenic focus, including fractional anisotropy (FA), axial diffusivity (AD), radial diffusivity (RD), and mean diffusivity (MD). Results are shown for healthy controls (CTRL, green), patients who achieved seizure freedom after surgery (SF, orange), and patients who did not achieve seizure freedom (Not-SF, cream). Boxes represent the interquartile range (IQR), central horizontal lines indicate the median, whiskers extend to 1.5 × IQR, and dots denote outliers. These measures reflect microstructural integrity and diffusion properties of ipsilateral hippocampal–thalamic pathways across clinical outcome groups.

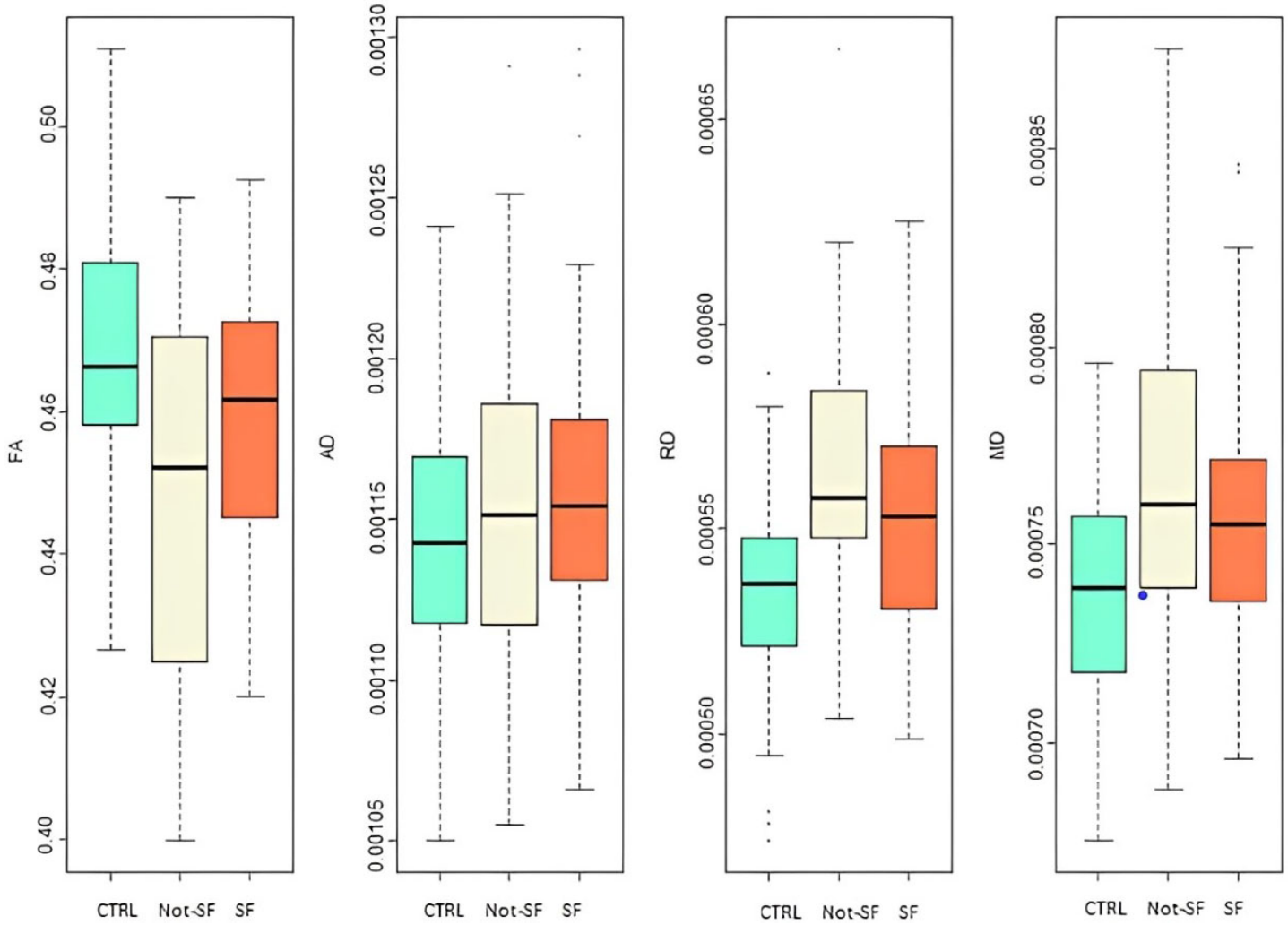

Fig. (7). Boxplots showing Diffusion Tensor Imaging (DTI) metrics between the hippocampus and the thalamus contralateral to the epileptogenic focus, including fractional anisotropy (FA), axial diffusivity (AD), radial diffusivity (RD), and mean diffusivity (MD). Comparisons are presented among healthy controls (CTRL, green), patients who achieved seizure freedom after surgery (SF, orange), and patients who did not achieve seizure freedom (Not-SF, cream). Boxes represent the interquartile range (IQR), horizontal lines indicate the median, whiskers extend to 1.5 × IQR, and dots correspond to outliers. These metrics characterize microstructural diffusion properties of contralateral hippocampal–thalamic pathways across outcome groups.

4.3. Diffusion Parameters

FA reduction in TLE patients, compared to controls, aligns with well-established literature linking FA declines to degenerative and demyelinating processes. This suggests that white matter integrity is compromised in TLE, potentially affecting functional connectivity and seizure propagation. These findings support the hypothesis of epilepsy as a network disorder, with structural connectivity changes playing a crucial role in its pathogenesis.

FA, AD, RD, and MD are established diffusion parameters for assessing TLE outcomes, applied hemispherically, individually, and in subcortical structures [57]. Our study demonstrated diffusion differences between seizure-free (SF) and not-seizure-free (Not-SF) patients, showing that outcome distinctions can be inferred from diffusion metrics in specific regions (Table **3**). This highlights the advantage of analyzing connections between structures rather than singular regions.

While the study's findings revealed significant differences across several pathways, these results must be interpreted with appropriate caution. Given that multiple ANOVA tests were conducted without a global correction (such as FDR or a secondary Bonferroni adjustment), there is an increased risk of Type I errors (false positives). Consequently, these *p*-values should be viewed as exploratory indicators of potential microstructural differences rather than definitive evidence of isolated pathological effects.

Boxplots illustrate that the interquartile range (IQR) and upper/lower limits in TLE patients show greater variation than controls. Discontinuous diffusion data were observed in Not-SF patients, particularly in FA, RD, and MD between the hippocampus and temporal pole ipsilateral to the epileptogenic focus (Fig. **4**), hippocampus and ipsilateral thalamus (Fig. **6**), and hippocampus and contralateral thalamus (Fig. **7**). Future studies may establish numerical diffusion metric thresholds for patient outcome classification.

MD levels in controls remained lower than in patients across all regions. Increased MD suggests elevated cerebrospinal fluid (CSF), indicating neurodegeneration due to compromised barriers restricting water molecule movement [60].

Multiple diffusion markers (FA, RD, MD) indicated white matter disruption between the hippocampus and ipsilateral temporal pole, reinforcing DTI's sensitivity to ipsilateral hemispheric changes in TLE [61]. In contrast, only a single metric (RD) distinguished hippocampus-temporal pole connectivity contralaterally, and FA for hippocampus-thalamus connectivity. Axial Diffusion (AD) failed to detect microscopic alterations, confirming previous findings [51, 38].

Seizure duration was not used as a covariate; however, FA differentiated hippocampus-thalamus connectivity among groups, consistent with prior studies showing FA reduction in the contralateral thalamus in medial structure sclerosis [62]. This suggests contralateral changes persist post-surgery, though their role in distinguishing SF and Not-SF groups remains unclear.

Increased RD and MD between the hippocampus and ipsilateral temporal pole suggest enhanced perpendicular water diffusion due to myelin sheath degradation [63].

An essential consideration in interpreting these findings is the impact of normal aging on white matter microstructure. It is well-documented that diffusion metrics such as FA decrease, while MD and RD increase, as part of the natural aging process. Given that our control group was significantly younger than the patient groups, the observed differences, particularly between controls and patients, may reflect a combination of MTLE-related pathology and age-related changes. Therefore, our results should be interpreted as exploratory associations at the group level rather than effects attributable solely to epilepsy or surgical outcome.

4.4. Clinical Implications

It is important to recognize the inherent heterogeneity within our Not-SF cohort. By combining patients with rare seizures (Engel II) and those with no improvement (Engel IV), we are analyzing a spectrum of surgical outcomes. While this approach allows for a preliminary comparison between 'responders' and 'non-responders', it may also average out specific microstructural patterns that could distinguish different degrees of surgical failure.

The focus of all scientific advances is to apply methods in a practical way to solve human problems, especially in the treatment of diseases. Surgery as a solution for reducing seizures and improving the quality of life of TLE patients has shown positive outcomes; however, hypotheses are still being raised, as there are cases of improvement and others of worsening, both at the behavioral and neurological levels [64].

In this context, recent evidence indicates that TLE is associated with dynamic reorganization of language and memory networks, characterized by presurgical functional hyperconnectivity and reduced structural connectivity, with partial reorganization after temporal lobectomy [65]. These findings support the view that microstructural properties captured by diffusion-based metrics may reflect relatively stable network constraints relevant to postoperative recovery.

Although the volume of the ipsilateral thalamus has reduced, as a site highly impacted by the disease [8], our findings indicate that knowing the volume is not enough to presuppose surgical recovery, but rather the diffusion dynamics analyzed in the white matter that surrounds the structures involved in TLE.

We believe that the data for the hippocampus-temporal pole ipsilateral ROI may contribute to patient selection in future studies, given that three diffusion parameters were able to detect differences between groups. Since TLE causes hippocampal sclerosis, it is crucial to assess whether the temporal pole is also affected, even after surgery [52, 38].

It is well known that DTI is a modern tool for analyzing neural network connectivity. This structural assessment modality has already been discussed regarding its utility in characterizing white matter alterations related to recovery for TLE patients undergoing surgery, showing advantages over other modalities such as fMRI and resting-state fMRI [54]. Knowing that the thalamus is the main node of early focal epilepsy before hippocampal atrophy [66], as a diagnostic indicator, we offer an early prognosis indicator.

Our program offers an advantage in terms of flexibility and applicability in potential new clinical contexts. The preliminary findings of this study may be promising but need to be validated in a larger, more preliminary cohort. Although our cohort of 77 patients is substantial compared to many DTI studies in the literature, it is important to emphasize that this work is exploratory in nature. This sample size is adequate for detecting significant group-level differences in white matter pathways associated with surgical outcomes, but it does not provide sufficient statistical power to support preliminary individual-level predictive modeling. Achieving this reality would make it possible to consider that further validation is required to explore how these group-level differences might eventually inform clinical perspectives.

5. LIMITATIONS

Raw diffusion data still pose a challenge for optimal utilization, considering that microscopic synaptic transfers occur in multiple directions, potentially leading to inaccuracies in the acquisition mechanism. In other words, the 32-gradient limitation must be taken into account.

A limitation of the methodology is that the processing of creating the specific white matter for the ROIs can be considered streamlined between ROI pairs beyond boundary structures such as 'seed' and 'target', suggesting an 'extra' surface to be included in the analysis (limitation of the developer). But as the program calculates the average of the diffusion parameters, such 'extra' surfaces of the streamlines have little weight on the total surface generated between ROIs. This can be identified in Fig. (**2**), with fibers remaining beyond those connecting ROIs, for example, between hippocampus and hippocampus; part of the greater forceps was included as fibers that structurally connect these regions, but in not all subjects is this tract projected.

Our study was unable to assess the threshold values of diffusion metrics as reference markers for individual recovery/seizure-free control. Instead, it only demonstrated that a diffusion metric can distinguish between a patient's improvement or deterioration. Therefore, as a future study, statistical techniques should be applied to establish this feasibility.

Considering the need for a multimodal analysis, it is possible to improve result accuracy by incorporating techniques such as resting-state fMRI, fMRI, EEG-fMRI, and other structural mapping methods, such as ODFs, to resolve crossing fibers [13]. Despite this, the results have proven to be highly consistent and satisfactory for a first study in this applied field.

The post-processing program we developed will be able to include new connectivity regions, such as gyri and other subcortical structures, enabling further advancements and future hypotheses.

This study has limitations inherent to its retrospective design. Imaging data were acquired over multiple years, potentially introducing variability. A primary limitation of this study is the modest sample size (n=77). While this cohort allows for reliable group comparisons, it is underpowered for building high-dimensional predictive models involving multiple imaging features. Attempting such modeling with the current dataset would carry a high risk of overfitting, where the model might describe random noise rather than true clinical patterns. Therefore, our results represent preliminary group-level associations rather than a validated clinical tool for individual prognostication.

Diffusion metrics are sensitive to acquisition parameters and tractography thresholds, which may underestimate microstructural abnormalities. Longitudinal postoperative DTI was not available for all patients, limiting the interpretation of dynamic network changes.

An additional potential limitation is the age difference between groups, as the control group was younger than the patient groups, which may confound diffusion measurements. However, the main comparison here was between seizure-free and not seizure-free patients and not between patients and controls. The DTI differences between patients with TLE and controls are well-established in the literature. Nevertheless, future studies should include age-matched controls or adjustment for age as a covariate.

Furthermore, the Not-SF group is heterogeneous, combining patients classified as Engel II, III, and IV. This grouping reflects the limited sample size available in this retrospective cohort but may obscure differences between distinct clinical outcomes. But the approach of comparing patients with Engel I outcome *versus* all other outcomes is not new and has been used consistently in a number of studies. It is true that combining these into a single "non-responder" category may obscure more nuanced, clinically meaningful relationships between diffusion metrics and the degree of surgical success. However, in clinical practice, the ideal outcome is Engel I, since having few seizures (Engel II) still impacts the patient's quality of life, precludes driving, and has several other consequences in people's lives. Furthermore, the approach of comparing seizure-free *versus* non-seizure-free patients is standard in the literature about epilepsy surgery.

The tractography-based connectivity analysis may include streamlines that extend beyond the intended ROI boundaries due to the method's intrinsic limitations. Although this effect was mitigated by averaging diffusion parameters across tracts, it may still introduce variability in the measurements.

A statistical limitation of this study is the lack of correction for multiple comparisons across the primary ANOVA tests. Conducting 20 separate tests increases the

likelihood of identifying significant differences by chance alone. Although post-hoc analyses were strictly corrected, the omission of a global correction for the main effects means that the validity of some significance values may be weakened. Future studies with larger cohorts should employ more stringent family-wise error correction methods to validate these preliminary associations.

Finally, a significant limitation of this study is the absence of a validated predictive model (*e.g.*, logistic regression or machine learning framework) to evaluate the sensitivity and specificity of these metrics for individual-level classification. Our findings are restricted to group-level differences and should be viewed as exploratory and hypothesis-generating.

CONCLUSION

This study strengthens the research on identifying group-level associations between white matter integrity and MTLE surgical outcomes. It was possible to identify structural differences between patients with poor seizure control after surgical treatment. The program functioned effectively for the intended analysis and was successfully applied to strategically selected regions.

Statistically significant differences between SF and Not-SF groups were observed through FA, RD, and MD markers in the ipsilateral regions (hippocampus-temporal pole connectivity). RD also identified differences in the contralateral hippocampus-temporal pole connectivity, while FA detected contralateral differences in hippocampus-thalamus connectivity.

The study reinforces that white matter changes are more pronounced in the hemisphere and temporal lobe ipsilateral to the epileptogenic focus. Connectivity between the hippocampus and other regions, such as the thalamus and temporal pole, proved crucial for analyzing post-surgery structural changes, as evidenced by FA reductions and increases in RD/MD. This study provides preliminary evidence using diffusion data for a detailed analysis of structural connectivity changes.

The methodology, combining tools such as Brainsuite, Tractconnect toolbox, and SVReg, enabled a preliminary, customized analysis, ensuring rigorous control over data processing and the evaluation of MTLE-affected connections.

The findings suggest that diffusion metrics may have the potential to suggest associations in patient recovery after MTLE surgery; however, they require validation in larger, prospective cohorts before clinical application. While promising, validation in a larger cohort is necessary to confirm clinical applicability.

A key limitation was the difficulty in establishing diffusion metric thresholds to associate individual surgical outcomes. Future studies should refine these analyses and integrate multimodal approaches, such as resting-state fMRI and EEG-fMRI, to provide a more comprehensive understanding of structural and functional changes in MTLE.

The project's next steps involve validating these results with additional tools, optimizing processing techniques, expanding the analysis to other brain regions, and applying statistical prediction models for new patients based on the findings.

These findings should be interpreted cautiously, as they reflect structural associations rather than definitive causal mechanisms.

AUTHORS' CONTRIBUTIONS

The authors confirm their contributions to the paper as follows: X.Í.C.P, C.F.: Study conception and design; M.A.M.K., Y.C.L.: Data collection; X.Í.C.P., C.B.M., C.F.: Analysis and interpretation of results; X.Í.C.P.: Draft manuscript preparation. All authors reviewed the results and approved the final version of the manuscript.

LIST OF ABBREVIATIONS

MRI	=	Magnetic Resonance Imaging
DTI	=	Diffusion Tensor Imaging
FA	=	Fractional Anisotropy
MD	=	Mean Diffusivity
AD	=	Axial Diffusivity
RD	=	Radial Diffusivity
TLE	=	Temporal Lobe Epilepsy
MTLE	=	Mesial Temporal Lobe Epilepsy
HS	=	Hippocampal Sclerosis
ROI	=	Region of Interest
TBSS	=	Tract-Based Spatial Statistics

ETHICAL STATEMENT

Ethical approval was obtained from the Institutional Review Board (IRB/Research Ethics Committee) formally named CEP-UNICAMP (Protocol CAAE:11634919.9.0000. 5404).

HUMAN AND ANIMAL RIGHTS

All human research procedures followed were in accordance with the ethical standards of the committee responsible for human experimentation (institutional and national), and with the Helsinki Declaration of 1975, as revised in 2013.

CONSENT FOR PUBLICATION

This retrospective observational study was conducted with patients' signed informed consent.

STANDARDS OF REPORTING

STROBE guidelines were followed.

AVAILABILITY OF DATA AND MATERIALS

The datasets generated and/or analyzed during the current study are available from the corresponding author upon reasonable request.

FUNDING

None.

CONFLICT OF INTEREST

The authors declare no conflict of interest, financial or otherwise.

ACKNOWLEDGEMENTS

This study was supported by the São Paulo State Research Support Foundation, FAPESP (grant number: 2022/04701-2).

REFERENCES

[1] Fisher RS, Cross JH, French JA, *et al*. Operational classification of seizure types by the International league against epilepsy: Position paper of the ILAE commission for classification and terminology. Epilepsia 2017; 58(4): 522-30. http://dx.doi.org/10.1111/epi.13670 PMID: 28276060

[2] da Costa JC. Neurobiological Foundations of Epilepsies: Clinical and Surgical Aspects (Portuguese Edition). Campinas: Lemos Editorial 1998.

[3] Wiebe S, Blume WT, Girvin JP, Eliasziw M. A randomized, controlled trial of surgery for temporal-lobe epilepsy. N Engl J Med 2001; 345(5): 311-8. http://dx.doi.org/10.1056/NEJM200108023450501 PMID: 11484687

[4] Waseem H, Vivas AC, Vale FL. MRI-guided laser interstitial thermal therapy for treatment of medically refractory non-lesional mesial temporal lobe epilepsy: Outcomes, complications, and current limitations: A review. J Clin Neurosci 2017; 38: 1-7. http://dx.doi.org/10.1016/j.jocn.2016.12.002 PMID: 28024732

[5] Johansen-Berg H, Behrens TEJ, Eds. Diffusion MRI: From quantitative measurements to in vivo neuroanatomy. Amsterdam: Elsevier Academic Press 2014. http://dx.doi.org/10.1016/C2011-0-07047-3

[6] Beaulieu C. The basis of anisotropic water diffusion in the nervous system – a technical review. NMR Biomed 2002; 15(7-8): 435-55. http://dx.doi.org/10.1002/nbm.782 PMID: 12489094

[7] Winklewski PJ, Sabisz A, Naumczyk P, Jodzio K, Szurowska E, Szarmach A. Understanding the physiopathology behind axial and radial diffusivity changes—what do we know? Front Neurol 2018; 9: 92. http://dx.doi.org/10.3389/fneur.2018.00092

[8] Alba-Ferrara LM, de Erausquin GA. What does anisotropy measure? Insights from increased and decreased anisotropy in selective fiber tracts in schizophrenia. Front Integr Nuerosci 2013; 7: 9. http://dx.doi.org/10.3389/fnint.2013.00009 PMID: 23483798

[9] Basser PJ, Pierpaoli C. A simplified method to measure the diffusion tensor from seven MR images. Magn Reson Med 1998; 39(6): 928-34. http://dx.doi.org/10.1002/mrm.1910390610 PMID: 9621916

[10] Turner R, Le Bihan D, Scott Chesnicks A. Echo-planar imaging of diffusion and perfusion. Magn Reson Med 1991; 19(2): 247-53. http://dx.doi.org/10.1002/mrm.1910190210 PMID: 1881311

[11] Tournier JD, Mori S, Leemans A. Diffusion tensor imaging and beyond. Magn Reson Med 2011; 65(6): 1532-56. http://dx.doi.org/10.1002/mrm.22924 PMID: 21469191

[12] Hagmann P, Jonasson L, Maeder P, Thiran JP, Wedeen VJ, Meuli R. Understanding diffusion MR imaging techniques: from scalar diffusion-weighted imaging to diffusion tensor imaging and beyond. Radiographics 2006; 26 (Suppl. 1): S205-23. http://dx.doi.org/10.1148/rg.26si065510 PMID: 17050517

[13] Hagmann P, Kurant M, Gigandet X, *et al*. Mapping human whole-brain structural networks with diffusion MRI. PLoS One 2007; 2(7): e597. http://dx.doi.org/10.1371/journal.pone.0000597 PMID: 17611629

[14] Pujol S, Wells W, Pierpaoli C, *et al*. The DTI Challenge: toward standardized evaluation of diffusion tensor imaging tractography for neurosurgery. J Neuroimaging 2015; 25(6): 875-82. http://dx.doi.org/10.1111/jon.12283 PMID: 26259925

[15] Bonilha L, Keller SS. Quantitative MRI in refractory temporal lobe epilepsy: relationship with surgical outcomes. Quant Imaging Med Surg 2015; 5(2): 204-24. http://dx.doi.org/10.3978/j.issn.2223-4292.2015.02.02 PMID: 25853080

[16] Hatton SN, Huynh KH, Bonilha L, *et al*. White matter abnormalities across different epilepsy syndromes in adults: an ENIGMA-Epilepsy study. Brain 2020; 143(8): 2454-73. http://dx.doi.org/10.1093/brain/awaa200 PMID: 32814957

[17] Thiebaut de Schotten M, ffytche DH, Bizzi A, *et al*. Atlasing location, asymmetry and inter-subject variability of white matter tracts in the human brain with MR diffusion tractography. Neuroimage 2011; 54(1): 49-59. http://dx.doi.org/10.1016/j.neuroimage.2010.07.055 PMID: 20682348

[18] Ahmadi ME, Hagler DJ Jr, McDonald CR, *et al*. Side matters: diffusion tensor imaging tractography in left and right temporal lobe epilepsy. AJNR Am J Neuroradiol 2009; 30(9): 1740-7. http://dx.doi.org/10.3174/ajnr.A1650 PMID: 19509072

[19] Concha L, Kim H, Bernasconi A, Bernhardt BC, Bernasconi N. Spatial patterns of water diffusion along white matter tracts in temporal lobe epilepsy. Neurology 2012; 79(5): 455-62. http://dx.doi.org/10.1212/WNL.0b013e31826170b6 PMID: 22815555

[20] Sun S, Tian M, Lin X, Zhao P, Zhang H, Liu W, *et al*. Disturbed white matter integrity on diffusion tensor imaging in young children with epilepsy. Clin Radiol 2024; 79(1): e119-26. http://dx.doi.org/10.1016/j.crad.2023.09.024 PMID: 37940443

[21] Dubey A, Kataria R, Sinha V. Role of diffusion tensor imaging in brain tumor surgery. Asian J Neurosurg 2018; 13(2): 302-6. http://dx.doi.org/10.4103/ajns.AJNS_226_16 PMID: 29682025

[22] Tung H, Pan SY, Lan TH, Lin YY, Peng SJ, Wang B, *et al*. Characterization of hippocampal–thalamic–cortical morphometric reorganization in temporal lobe epilepsy. Front Neurol 2022; 12: 810186. http://dx.doi.org/10.3389/fneur.2021.810186 PMID: 35222230

[23] Statistical Parametric Mapping. 2020. Available from: https://www.fil.ion.ucl.ac.uk/spm/

[24] Yildirim MS, Stepponat R, Fischmeister FPS, *et al*. Decreased Structural Connectivity Between Thalamic Nuclei and Hippocampus in Temporal Lobe Epilepsy—A Diffusion Tensor Imaging-Based Study. Eur J Neurol 2025; 32(1): e70040. http://dx.doi.org/10.1111/ene.70040 PMID: 39797565

[25] Barron DS, Fox PM, Laird AR, Robinson JL, Fox PT. Thalamic medial dorsal nucleus atrophy in medial temporal lobe epilepsy: A VBM meta-analysis. Neuroimage Clin 2013; 2: 25-32. http://dx.doi.org/10.1016/j.nicl.2012.11.004 PMID: 24179755

[26] Fallahi A, Nazem-Zadeh MR, Hoseini-Tabatabaei N, Mehvari Habibabadi J, Hashemi Fesharaki SS, Soltanian-Zadeh H. Language and Memory Network Alterations in Temporal Lobe Epilepsy: A Functional and Structural Connectivity Study. AJNR Am J Neuroradiol 2025; 46(9): 1953-62. http://dx.doi.org/10.3174/ajnr.A8737 PMID: 40081848

[27] Holmes MJ, Yang X, Landman BA, *et al*. Functional networks in temporal-lobe epilepsy: a voxel-wise study of resting-state functional connectivity and gray-matter concentration. Brain Connect 2013; 3(1): 22-30. http://dx.doi.org/10.1089/brain.2012.0103 PMID: 23150897

[28] Park KM, Kim SE, Shin KJ, *et al*. Effective connectivity in temporal lobe epilepsy with hippocampal sclerosis. Acta Neurol Scand 2017; 135(6): 670-6. http://dx.doi.org/10.1111/ane.12669 PMID: 27558524

[29] Abel TJ, Woodroffe RW, Nourski KV, *et al*. Role of the temporal pole in temporal lobe epilepsy seizure networks: an intracranial electrode investigation. J Neurosurg 2018; 129(1): 165-73.

http://dx.doi.org/10.3171/2017.3.JNS162821 PMID: 29027858
[30] Cendes F, Sakamoto AC, Spreafico R, Bingaman W, Becker AJ. Epilepsies associated with hippocampal sclerosis. Acta Neuropathol 2014; 128(1): 21-37. http://dx.doi.org/10.1007/s00401-014-1292-0 PMID: 24823761
[31] de Bézenac CE, Leek N, Adan GH, *et al*. Subcortical Alterations in Newly Diagnosed Epilepsy and Associated Changes in Brain Connectivity and Cognition. Hum Brain Mapp 2024; 45(16): e70069. http://dx.doi.org/10.1002/hbm.70069 PMID: 39508641
[32] Fonteijn HMJ, Norris DG, Verstraten FAJ. Exploring the anatomical basis of effective connectivity models with DTI-based fiber tractography. Int J Biomed Imaging 2008; 2008(1): 423192. http://dx.doi.org/10.1155/2008/423192 PMID: 18483617
[33] Caciagli L, Paquola C, He X, *et al*. Disorganization of language and working memory systems in frontal *versus* temporal lobe epilepsy. Brain 2023; 146(3): 935-53. http://dx.doi.org/10.1093/brain/awac150 PMID: 35511160
[34] Ji GJ, Fox MD, Morton-Dutton M, *et al*. A generalized epilepsy network derived from brain abnormalities and deep brain stimulation. Nat Commun 2025; 16(1): 2783. http://dx.doi.org/10.1038/s41467-025-57392-7 PMID: 40128186
[35] Olejnik A, Bala A, Rejner W, *et al*. Gray matter abnormalities and memory impairment in left mesial temporal lobe epilepsy. Front Hum Neurosci 2025; 19: 1554091. http://dx.doi.org/10.3389/fnhum.2025.1554091 PMID: 40893696
[36] Urquia-Osorio H, Pimentel-Silva LR, Rezende TJR, *et al*. Superficial and deep white matter diffusion abnormalities in focal epilepsies. Epilepsia 2022; 63(9): 2312-24. http://dx.doi.org/10.1111/epi.17333 PMID: 35707885
[37] Campos BM, Coan AC, Beltramini GC, *et al*. White matter abnormalities associate with type and localization of focal epileptogenic lesions. Epilepsia 2015; 56(1): 125-32. http://dx.doi.org/10.1111/epi.12871 PMID: 25545559
[38] Keller SS, Cresswell P, Denby CE, Wieshmann UC, Brennan P, Roberts N. Concomitant fractional anisotropy and volumetric abnormalities in temporal lobe epilepsy: cross-sectional evidence for progressive neurologic injury. Epilepsia 2012; 53(4): 651-60. http://dx.doi.org/10.1111/j.1528-1167.2012.03418.x PMID: 22360759
[39] Gouveia FV, Warsi NM, Suresh H, Matin R, Ibrahim GM. Neurostimulation treatments for epilepsy: Deep brain stimulation, responsive neurostimulation and vagus nerve stimulation. Neurotherapeutics 2024; 21(3): e00308. http://dx.doi.org/10.1016/j.neurot.2023.e00308 PMID: 38177025
[40] François L, Romagnolo A, Luinenburg MJ, *et al*. Identification of gene regulatory networks affected across drug-resistant epilepsies. Nat Commun 2024; 15(1): 2180. http://dx.doi.org/10.1038/s41467-024-46592-2 PMID: 38467626
[41] Elizalde Acevedo B, Kochen S, Alba-Ferrara L, Bendersky M. Reorganization of pragmatic language networks in patients with temporal lobe epilepsy. Clin Neurophysiol 2025; 170: 194-205. http://dx.doi.org/10.1016/j.clinph.2024.12.012 PMID: 39742834
[42] Shattuck DW, Leahy RM. BrainSuite: cortical surface extraction. Los Angeles: UCLA Brain Mapping Center 2001.
[43] UCLA. Welcome to the BrainSuite Website. 2021. Available from: http://brainsuite.org/
[44] Andersson JLR, Graham MS, Zsoldos E, Sotiropoulos SN, Filippini N, Bastiani M. Incorporating outlier detection and replacement into a non-parametric framework for movement and distortion correction of diffusion MR images. Neuroimage 2016; 141: 556-72. http://dx.doi.org/10.1016/j.neuroimage.2016.06.058 PMID: 27393418
[45] Yeh FC, Zaydan IM, Suski VR, *et al*. Differential tractography as a track-based biomarker for neuronal injury. Neuroimage 2019; 202: 116131. http://dx.doi.org/10.1016/j.neuroimage.2019.116131 PMID: 31472253
[46] Bhushan C, Haldar JP, Choi S, Joshi AA, Shattuck DW, Leahy RM. Co-registration and distortion correction of diffusion and anatomical images based on inverse contrast normalization. Neuroimage 2015; 115: 269-80. http://dx.doi.org/10.1016/j.neuroimage.2015.03.050 PMID: 25827811
[47] Chong M. TracConnect MATLAB Toolbox. 2014. Available from: https://neuroimage.usc.edu/neuro/Resources/TractConnect/
[48] R: A Language and Environment for Statistical Computing. 2020. Available from: https://www.R-project.org/
[49] Otte WM, van Eijsden P, Sander JW, Duncan JS, Dijkhuizen RM, Braun KPJ. A meta-analysis of white matter changes in temporal lobe epilepsy as studied with diffusion tensor imaging. Epilepsia 2012; 53(4): 659-67. http://dx.doi.org/10.1111/j.1528-1167.2012.03426.x PMID: 22379949
[50] Sasaki T, Makris N, Shenton ME, *et al*. Structural connectivity of cytoarchitectonically distinct human left temporal pole subregions: a diffusion MRI tractography study. Front Neuroanat 2023; 17: 1240545. http://dx.doi.org/10.3389/fnana.2023.1240545 PMID: 38090110
[51] Giacomini L, de Souza JPSA, Formentin C, *et al*. Temporal lobe structural evaluation after transsylvian selective amygdalohippocampectomy. Neurosurg Focus 2020; 48(4): E14. http://dx.doi.org/10.3171/2020.1.FOCUS19937 PMID: 32234992
[52] González-Zacarías C, Choi S, Vu C, *et al*. Chronic anemia: The effects on the connectivity of white matter. Front Neurol 2022; 13: 894742. http://dx.doi.org/10.3389/fneur.2022.894742 PMID: 35959402
[53] Javidi SS, He X, Ankeeta A, *et al*. Edge-wise analysis reveals white matter connectivity associated with focal to bilateral tonic–clonic seizures. Epilepsia 2024; 65(6): 1756-67. http://dx.doi.org/10.1111/epi.17960 PMID: 38517477
[54] Zhang Y, Liu Z, Dou W, *et al*. Study of the microstructure of brain white matter in medial temporal lobe epilepsy based on diffusion tensor imaging. Brain Behav 2023; 13(4): e2919. http://dx.doi.org/10.1002/brb3.2919 PMID: 36880299
[55] Elliott CA, Gross DW, Wheatley BM, Beaulieu C, Sankar T. Longitudinal hippocampal and extra-hippocampal microstructural and macrostructural changes following temporal lobe epilepsy surgery. Epilepsy Res 2018; 140: 128-37. http://dx.doi.org/10.1016/j.eplepsyres.2018.01.008 PMID: 29331847
[56] Alizadeh M, Kozlowski L, Muller J, *et al*. Hemispheric regional-based analysis of diffusion tensor imaging and diffusion tensor tractography in patients with temporal lobe epilepsy and correlation with patient outcomes. Sci Rep 2019; 9(1): 215. http://dx.doi.org/10.1038/s41598-018-36818-x PMID: 30659215
[57] Concha L, Beaulieu C, Collins DL, Gross DW. White-matter diffusion abnormalities in temporal-lobe epilepsy with and without mesial temporal sclerosis. J Neurol Neurosurg Psychiatry 2009; 80(3): 312-9. http://dx.doi.org/10.1136/jnnp.2007.139287 PMID: 18977826
[58] Lim SC, Oh J, Hong BY, Lim SH, Kim JH, Kim H. Changes in the brain in temporal lobe epilepsy with unilateral hippocampal sclerosis: an initial case series. Healthcare (Basel) 2022; 10(9): 1648. http://dx.doi.org/10.3390/healthcare10091648 PMID: 36141260
[59] Nguyen D, Vargas MI, Khaw N, *et al*. Diffusion tensor imaging analysis with tract-based spatial statistics of the white matter abnormalities after epilepsy surgery. Epilepsy Res 2011; 94(3): 189-97. http://dx.doi.org/10.1016/j.eplepsyres.2011.02.001 PMID: 21377331
[60] García-Pallero MA, Hodaie M, Zhong J, *et al*. Prediction of laterality in temporal lobe epilepsy using white matter diffusion metrics. World Neurosurg 2019; 128: e700-8. http://dx.doi.org/10.1016/j.wneu.2019.04.238 PMID: 31059852
[61] Winston GP, Vos SB, Caldairou B, *et al*. Microstructural imaging in temporal lobe epilepsy: Diffusion imaging changes relate to reduced neurite density. Neuroimage Clin 2020; 26: 102231.

http://dx.doi.org/10.1016/j.nicl.2020.102231 PMID: 32146320
[62] Winston GP, Stretton J, Sidhu MK, Symms MR, Duncan JS, Ourselin S, *et al*. Progressive white matter changes following anterior temporal lobe resection for epilepsy. Neuroimage Clin 2014; 4: 190-200. http://dx.doi.org/10.1016/j.nicl.2013.12.004 PMID: 24392306
[63] de Souza JPSAS, Ayub G, Pereira PC, *et al*. Fractional anisotropy of the optic radiations correlates with the visual field after epilepsy surgery. Neuroradiology 2019; 61(12): 1425-36. http://dx.doi.org/10.1007/s00234-019-02281-2 PMID: 31494681
[64] de Souza JPSAS, Ayub G, Nogueira M, *et al*. Temporopolar amygdalohippocampectomy: seizure control and postoperative outcomes. J Neurosurg 2020; 134(3): 1044-53. http://dx.doi.org/10.3171/2019.10.JNS192022 PMID: 32413857
[65] Fırat Z, Ekinci G, Schulz D. Diffusion tensor imaging with tractography to predict memory deficits in patient groups with temporal lobe lesions. J Clin Neurosci 2025; 140: 111526. http://dx.doi.org/10.1016/j.jocn.2025.111526 PMID: 40752303
[66] Revell AY, Jaskir M, Lucas A, *et al*. White matter signals reflect information transmission between brain regions during seizures. Brain 2026; 149(1): 77-89. http://dx.doi.org/10.1093/brain/awaf444 PMID: 41340548